

Document downloaded from:

<http://hdl.handle.net/10251/206709>

This paper must be cited as:

Cifuentes, G.; Germain, I.; Garrido, B.; Cifuentes-Cabezas, M.; Orrego, P.; Gencico, I.; Pino, E.... (2022). Tetra-uranium fluoride electrowinning by electro-electrodialysis cell (EED). *Separation and Purification Technology*. 281:1-7.
<https://doi.org/10.1016/j.seppur.2021.119833>



The final publication is available at

<https://doi.org/10.1016/j.seppur.2021.119833>

Copyright Elsevier

Additional Information

Tetra-uranium fluoride electrowinning by electro-electrodialysis cell (EED)

*Gerardo Cifuentes¹, Ignacio Germain², Belén Garrido¹, Magdalena Cifuentes-Cabezas³,
Pedro Orrego², Iván Genticó¹, Eduardo Pino⁴, Cristian Calderón⁴*

¹*Department of Metallurgical Engineering, University of Santiago of Chile (USACH), Avda. L.B. O'Higgins
3363, Estación Central, Santiago, Chile, gerardo.cifuentes@usach.cl*

²*Department of Nuclear Materials, Chilean Nuclear Energy Commission (CCHEN), Amunátegui 95, Santiago,
Chile*

³*Research Institute for Industrial, Radiophysical and Environmental Safety (ISIRYM), Department of Chemical
and Nuclear Engineering, Universitat Politècnica de València (UPV), C/Camino de Vera s/n, 46022 Valencia,
Spain.*

⁴*Department of Environmental Science, University of Santiago of Chile (USACH), Avda. L.B. O'Higgins 3363,
Estación Central, Santiago, Chile.*

Abstract

This work presents a novel electro-electrodialysis (EED) system for laboratory-scale uranium electrowinning based on a simple process of reactive electro dialysis of solutions of uranium (VI) oxide (UO_3) dissolved in aqueous hydrofluoric acid (HF), leading to the formation of deposits of uranium tetrafluoride (UF_4). For stainless steel cathodes, the best operating conditions for a concentration of 25 g/L for uranium were $i = 40 \text{ A/m}^2$, $T = 40^\circ\text{C}$ and 18 L/h recirculation flowrate. The specific energy consumption (W) and current efficiency (ρ) for tetra uranium fluoride electrowinning was 4500 kWh/kg and 10.15%. When the cathodic metal was changed from stainless steel to aluminium, seeking to optimize the system, improved values of W and ρ were achieved (645 kWh/kg and 68%, respectively).

In the EED cells, the release of gaseous hydrogen is significantly lower for aluminum, due to its lower exchange current density (i_0), with a magnitude of 10^{-7} A/m^2 . On the contrary, a considerable release of gaseous hydrogen is observed when the stainless-steel cathode is used, mainly due to the H^+/H_2 reaction being catalysed by the stainless steel, inducing an increase in the acid consumption rate, devoting most of the energy consumed by the system in the proton reduction reaction. Polarization cathodic curves indicate that uranium has an estimate resting potential close to that of aluminium, which is -0.89 V .

Finally, by chemical analysis (X-ray mass diffraction), UF_4 and hydrated UF_4 , were identified as the main components of the electrodeposited product

Keywords: Electro-electrodialysis, Electrowinning, Uranium tetrafluoride

1. Introduction

Radioactive materials usually take the spotlight based on their relevance as sources of energy for varied applications [1]. In particular, a considerable amount of attention is placed on uranium as one of the most known radioactive materials currently in use [2]. Interestingly, not much attention is drawn to the complete nuclear fuel cycle of uranium, which includes all the processes that the uranium undergoes, from its ore extraction to its use in a reactor and its latter elaboration or storage [3].

The concentration and purification of uranium-rich ores is a complex undertaking [4], involving several processes such as: i) steps associated with the discovery of suitable deposits for mining, quality sorting of the obtained ores, ii) milling and processing of the raw material and iii) sequential physico-chemical processing of the material, in both dry and wet processes, to achieve a low yield of uranium. This is an issue that arises from the initial low concentration of uranium found in the ores deemed as suitable for processing, with a uranium content lower than 20%, mainly in the form of uranium oxide [1]. Coupled with the intricacies inherent in the uranium mining process, important considerations need to be taken to establish adequate and traceable radiological control [5], to control the generation of radioactive waste according to the governmental regulations in place during the radioactive material processing [5].

On the uranium enrichment process, the treatment of the ore is produced by two main routes, an acid route, and an alkaline route [6], both dealing with successive steps of dissolution, neutralization, precipitation, and redissolution, which involve the treatment of large volumes of leachates which require treatment and concentration to obtain the desired material.

To achieve the desired concentration of uranium in the wet stages of the ore treatment, novel strategies need to be considered to optimize the use of aqueous resources as well as to improve the

amount and purity of the uranium [7], [8]. Considering the above-mentioned limitations, electrochemical processes have usually been considered as ideal candidates for processes of selective separation of chemical species [9], [11]. The complementary use of several electrochemical techniques, as well as other physicochemical processes, can lead to the development of cost-effective systems with good recovery performance of the desired chemical species.

The Chilean Commission of Nuclear Energy (CCHEN) developed novel Lab-scale electrowinning cells [12], which use membranes as a separator of catholyte and anolyte fluids. In the latter case, it has been stressed that the nature of the anodic material has shown itself to be highly relevant. Even though membrane-cells were first proposed for the recovery of copper [12], [14], its use has been extended to several applications [15], [16], [17], [18], [19], [20], [21], [22]. The present work describes the experimental development of a uranium electrowinning cell design aiming to develop a laboratory-scale cell based on reactive electro dialysis. To achieve these objectives, a two-compartment cell (one for cathode and catholyte and another for anode and anolyte) operating under continuous flow regime was developed.

In the CCHEN institute, several studies have been carried out for the extraction of uranium, based on the use of electro-electrodialysis (EED) processes. This method consists of a combination of electrolysis and electro dialysis, which allows to obtain different chemical products in two electrolytes (anolyte and catholyte) separated by one or more membranes, anion and/or cation exchange ones, using electric current between two electrodes (anode and cathode) as the driving force for the process to take place under different experimental conditions, such as substrate concentration, acidity, temperature and so on [23]. EED systems have found considerable use in

water purification processes [17], organic and inorganic acids and the recovery of bases [22], as well as treatments for metal recovery from liquid samples [10].

The current iteration of the system, presented in this work, corresponds to a reactive electro-electro dialysis system (REED). This system was used for electrowinning of UF_4 , to reduce the uranium in solution as solid UF_4 , from UO_3 dissolved in HF [24-26]. The reduction of uranium occurs in the cathode [27], equation (1); and therefore, gaseous hydrogen is produced, equation (2). The anode contains H_2SO_4 1M and the reaction is the water hydrolysis, equation (3). **¡Error! No se encuentra el origen de la referencia.** show a diagram of the REED system.

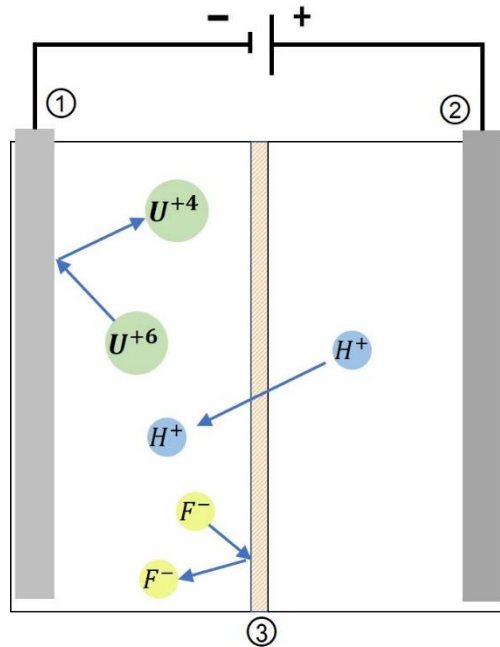
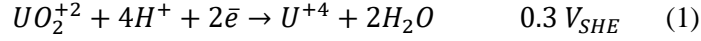
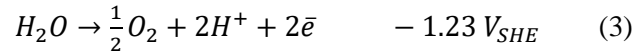


Figure 1. Schematic representation of a reactive electro-electro dialysis cell (REED). (1) Anodic electrode. (2) Cathodic electrode. (3) Cationic membrane.

The cathodic half reactions with standard hydrogen potentials electrode (SHE) are:



The anodic half reactions with standard potentials are:



Uranium tetrafluoride (UF₄) is a solid green crystal, and is used primarily as a reagent for the manufacture of a nuclear fuel element. The electrochemical production of UF₄ is well documented [1] and several strategies have been tested throughout the years; one of the most well-known processes associated with the production of UF₄ is the EXCER process [29]. In this process, a solution of uranyl nitrate (UO₂(NO₃)₂) is put into contact with a cationic resin, from this, the product, uranyl fluoride (UO₂F₂) which is then thoroughly reduced to hydrated UF₄. The proposed electrochemical reaction taking place in our studies (vide supra), and the ease of use provided by the proposed REED system, coupled with properties of UF₄ such as thermal stability and low solubility in water [25], allow for the development of a simple and efficient system which can be easily escalated for the development of large-scale processes for purification and concentration of uranium compounds.

2. Experimental procedure

¡Error! No se encuentra el origen de la referencia.2 (Above) show the reactive electro-dialysis system from UF_4 extraction, with the configuration deployed at a workbench scale.

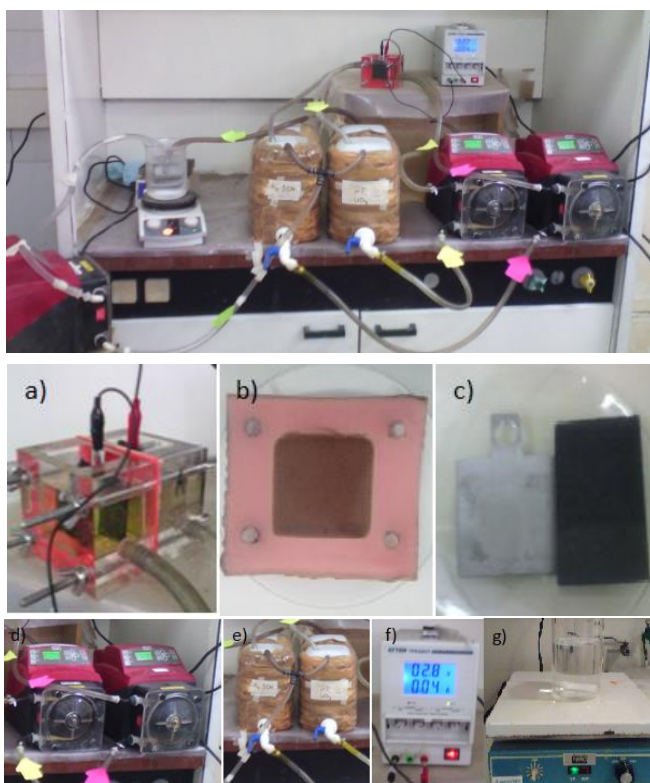


Figure 2. (Above) Complete view of the reactive electro-electrodialysis (REED) system for UF_4 extraction. (Below) Detailed view of the REED components. a) electrolytic cell, b) membrane, c) cathode and anode d) pumps, e) solution containers, f) DC power supply and g) heating plate.

The system consists of a homemade two-compartment acrylic cell (Fig. 2.a) separated by a sulphurated polystyrene cationic membrane (Fig. 2.b), the catholyte and anolyte solutions were recirculated. The cathode was made of stainless steel, its dimensions were $4.9 \times 4.9 \times 0.1$ cm, and the anode was made of graphite, and was $6 \times 3 \times 1$ cm (Fig. 2.c).

The cell is connected to two drums that contain 25 g/L UO_3 with HF (1M), and the other with H_2SO_4 (1M) (¡Error! No se encuentra el origen de la referencia..d), each drum has a 10L capacity, through which hot water circulates, coming from a heater, heating the solutions to 20, 30 and 40°C.

Peristaltic pumps with a flow rate of 20 L/h (¡Error! No se encuentra el origen de la referencia..e), and a DC model ATTEN TPR3003T power supply were used (¡Error! No se encuentra el origen de la referencia..f), with a current density of 40, 80 and 100 A/m². The cell operated at normal pressures in all the experimental conditions tested.

All experiments were carried out at least by triplicate, unless otherwise stated. For a given set of replicates, data was deemed adequate when no differences larger than 20% between them were observed.

3. RESULTS AND DISCUSSIONS

After five hours of continuous work of the REED cell, an inspection of the stainless steel cathode allowed for the visualization of a greenish fine layer of UF_4 , with a discernible concentration of the deposited UF_4 at the center of the cathode, deposits that decrease when moving toward the outer limits of the cathode Fig. 3.



Figure 3. Tetrauranium fluoride electrodeposited on a stainless-steel bed

Regarding the amount of UF_4 deposits obtained in the cycle of operation, to standardize the mass determination, the mass of UF_4 deposit obtained was estimated after 18 experiments performed in different conditions of temperature, UO_3 concentration and current density. The results of UF_4 extracted mass are shown in Fig. 4.

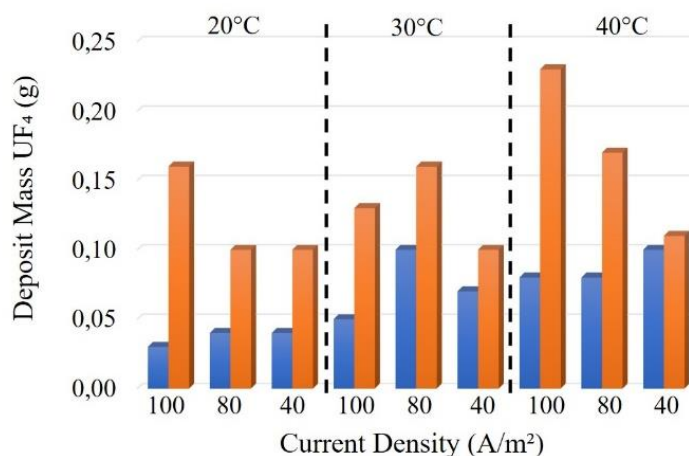


Figure 4. UF_4 deposit mass vs. current density on a REED cell equipped with a stainless steel cathode. The dashed line delimits the different operating catholyte temperature tested (20, 30 and 40 °C). For each pair of bars, the bars on the left represent mass of deposit obtained at a UO_3 concentration of 15 g/L, whereas the bars to the right correspond to mass of deposit obtained at a UO_3 concentration of 25 g/L.

At the lowest temperature tested (20 °C), when the system is operating at the lowest concentration of the uranium solutions tested (15 g/L), no significative differences are observed in the deposited mass of UF_4 with the increase of the current density. On the contrary, at the highest uranium concentration (25 g/L) tested, a 50% increase on the amount of deposited UF_4 is observed at 100

A/m² current density, compared to 80 A/m² and 40 A/m². At the largest current density tested, the increase of Uranium solution concentration induces almost a tenfold increase in UF₄ deposit, whereas at 80 A/m² and 40 A/m², a twofold increase is observed. An intermediate increase of temperature in the system (30 °C), overall improves the UF₄ deposit performance of the system at 15 g/L uranium solution concentration, irrespective of the current density of the system. At 25 g/L uranium solution, no striking differences are overall observed in the mass of UF₄ deposits, compared to that observed at 20 °C. Interestingly at 30 °C, the difference in UF₄ deposit efficiency is lessened between 15 g/L and 25 g/L uranium solutions. At the highest temperature tested (40 °C), a significant improvement on the mass of UF₄ deposited is observed at 25 g/L uranium solution, where the maximum UF₄ deposit efficiency, from all the conditions tested, is observed, where the highest amount of extracted mass was 0.22 g, achieved at 40 °C, 100 A/m² current density and a 25 g/L uranium concentration.

The observations based on the data presented in Fig. 4, can be explained by considering the impact of the current density of the system on the ability to create nucleation centers during the electrodeposition stage on the EED process [13]. For the nucleation process, the current density controls the rate at which the metal crystals are formed as well as their growth kinetics, with lower current densities leading to the formation of a reduced number of highly ordered nucleation centers, while high current densities lead to the formation of a larger number of nucleation centers with a more unstructured disposition leading to more porous deposits. As expected, the use of high concentration of UO₃ (25 g/L) and high current densities, leads to the highest values of UF₄ deposited mass due to the formation of a large number of nucleation centers able to grow on the surface to grow until the final mass of deposited UF₄ is achieved.

When the temperature influence is considered [30], it can be observed that irrespective of the concentration of UO_3 , the deposition of UF_4 is improved with the increase of temperature. From this it can be inferred that the formation of the UF_4 deposited is not only favoured by the large number of nucleation centers induced by the high current densities, but also by the increased size of the metal crystals led by the increase in temperature. Besides this, the increase in temperature can induce and improved transport of metal mass to the surface of the electrode, due to increased solubility and conductivity of the solution.

Regarding the data obtained at 30 °C, the behaviour of the systems appears to be rather different compared to that observed at 20° and 40 °C. Particularly considering that at 30°, an intermediate condition appears, where the largest amount of deposited material (irrespective of UO_3 concentration) is achieved at a lower current density value (80 A/m²). The most likely explanation for the observed differences is the presence of hydrogen occlusion mechanisms [31] that can be patent at lower temperatures, having a direct impact in the amount of deposited material, due to the large amounts of gaseous hydrogen being trapped in the newly formed metallic structures. The hydrogen occlusion might have a lessened impact in our systema operating at 40 °C, due to the decreased solubility of hydrogen and the increased evolution of gas from the system. Particularly, the conditions achieved at 30 °C acting as a “tipping point” for the influence of the hydrogen occlusion phenomena.

The determination of the theoretical deposited mass (M_T) at the cathode was made using by Faraday equation (4) and the current efficiency is calculated by the equation (5):

$$M_T = \frac{I \cdot P \cdot M}{n \cdot F} \quad (4)$$

$$\rho = \frac{M_R}{M_T} \quad (5)$$

Where in eq. 4, I is the current, P is the process elapsed time, M is the deposited substance molar mass. n and F are substance moles and faraday constant respectively.

With the real (M_R) and theoretical mass, the current efficiency (ρ) was calculated, Fig. 5 shows the current efficiency of every operational condition.

Now, with equation (6) the energy needed to extract one kilogram of uranium (W) can be calculated:

$$W = \frac{U_{terminal} \cdot I \cdot t}{M_R} \quad (6)$$

$U_{terminal}$ is the potential applied to the system, I correspond to the current and t is the time required for the deposition of a given amount of UF_4

Fig. 5 shows data obtained for the evaluation of the correlation between current efficiency and current density in the REED system.

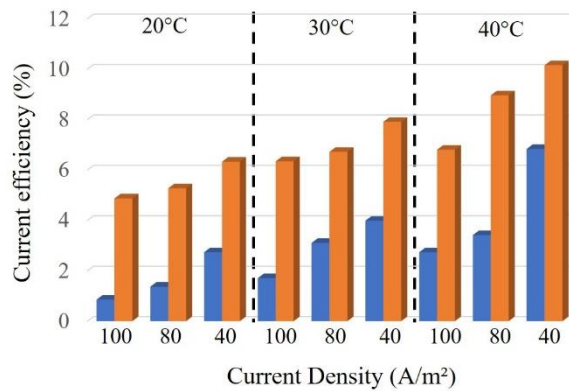


Figure 5. Current efficiency vs. current density on a REED cell equipped with a stainless steel cathode. The dashed line delimits the different operating catholyte temperature tested (20, 30 and 40 °C). For each pair of bars, the bars on the left represent mass of deposit obtained at a

UO₃ concentration of 15 g/L, whereas the bars to the right correspond to mass of deposit obtained at a UO₃ concentration of 25 g/L.

From the data in Fig. 5, interesting observations can be made. First, overall current efficiency increases with the increase of the operating temperature in the system, with the estimated current density increasing almost linearly with the increase in temperature from 20 to 40 °C, irrespective of the uranium solution concentration employed. Similarly, in all the experimental conditions considered, the largest current efficiency is achieved when the system is operating with the catholyte at the highest uranium concentration studied (25 g/L). Also, in all of the conditions tested, lower current density induces the highest current efficiency, irrespective of the temperature of the system and the concentration of uranium solution. The observed increase in current efficiency with the applied current density into the system, is concomitant with the increase on the UF₄ deposited mass, higher current density indicates an enhanced supply of electrochemically active species (i.e. UO₃) to the electrode surface. This is further supported by the increase in temperature, which indicates that the mass transfer coefficients of the electroactive species are increasing thus enhancing the deposition process. Another factor that might be contributing to the current efficiency trend is the minimization of potentially competing reactions taking place during the deposition process.

Regarding the relationship between the specific energy consumption and current density for the deposition of UF_4 in the REED cell, from the data collected in Fig. 5, the specific energy consumption of the systems under study was calculated. Fig. 6 shows that the efficiency is inversely proportionate to the specific energy consumption. At low temperatures ($20\text{ }^\circ\text{C}$), significant differences are observed in specific energy consumption, where comparisons are made between the two concentrations of UO_3 tested (15 g/L and 25 g/L). These differences are further reduced with the increase in temperature of up to $40\text{ }^\circ\text{C}$, where an overall decrease in specific energy consumption is observed at both UO_3 concentrations. Concomitant with this, the more impactful decrease is observed at $15\text{ g/L } UO_3$ solutions.

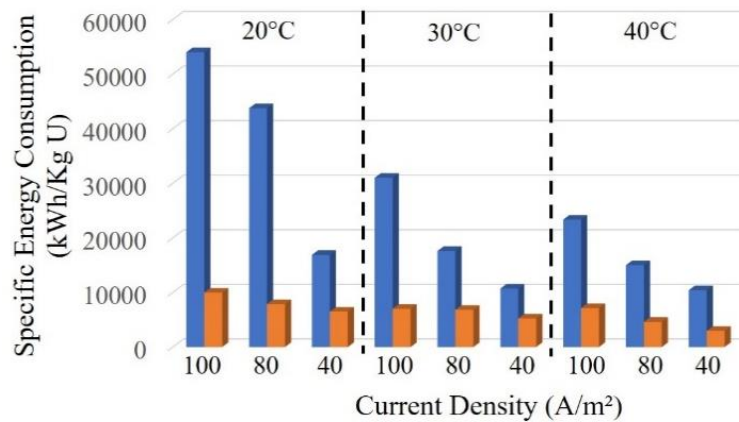


Figure 6. Specific energy consumption vs. current density on a REED cell equipped with a stainless steel cathode. The dashed line delimits the different operating catholyte temperature tested (20 , 30 and $40\text{ }^\circ\text{C}$). For each pair of bars, the bars on the left represent mass of deposit obtained at a UO_3 concentration of 15 g/L , whereas the bars to the right correspond to mass of deposit obtained at a UO_3 concentration of 25 g/L .

After the data analysis and with the linear regression of the results presented in 5, model 1 was created, (current efficiency, with an R^2); and with the results of 6, model 2 was created, (specific consumption, with an R^2).

$$\rho = -0.04 \cdot i + 0.146 \cdot T + 0.407 \cdot C - 4.5 \quad (7)$$

$$W = 4,025 \cdot V - 194 \cdot i - 562 \cdot T - 1,513 \cdot C + 36,324 \quad (8)$$

In a REED system, the evaluation and control of parameters such as current density, current efficiency (and hence cell voltages) is no trivial matter, given the fact that the accurate manipulation of the efficiency of the system has direct impact on the long-term operation of the system and control of the cost associated with the deposition of the chosen uranium compounds. At a given operational set of the aforementioned parameters, the conditions under which the REED cell operates, such as electrode configuration (geometries and materials), uranium and acid concentration, temperature, agitation, can have a direct impact on the power required to deposit a set amount of Uranium-rich material. From this, the specific consumption estimated in the operational conditions considered indicate that the configuration of the REED cell provides adequate operational conditions to achieve an efficient production, considering the simplicity of the proposed system.

One of the most important considerations to be taken into account for the operation of a system based on electrochemical processing of solution of considerable acidity, is that it relies on the behaviour of the electrodes used in a given system design. In particular, for the system proposed in this work, the behaviour of the cathodes is relevant, taking into consideration that this electrode is in direct contact with HF, and any variation in the behaviour of the electrode due to undesired processes such as corrosion of the electrode or other secondary reactions can directly affect the capacity of the system to maintain the desired current densities and efficiencies required for adequate operational conditions.

Due to the overall low current efficiencies estimated for the REED system studied, experiments with different cathodes were performed, to assess the impact of the cathodic material on the performance of the REED system, and to be able to establish further considerations that can lead to improvement on the UF₄ deposition process. To achieve this goal, experiments were performed at a limited set of conditions, previously estimated for the system operating with stainless steel cathodes, namely, a temperature of 40 °C, 40 A/m² of current density and a uranium concentration of 25 g/L. The metallic material tested for comparison against stainless steel were aluminium, Monel (a nickel/copper alloy) and Inconel (a nickel/chromium alloy) [32], [33]. Table 1 shows the results for current efficiency and specific energy consumption.

Table 1: Results for current efficiency and specific energy consumption using other cathodic metals for the electrodeposition of UF₄ in the studied REED cell.

	Metal			
	Stainless steel	Aluminium	Monel	Inconel
ρ (%)	10.15	68.29	6.83	17.07
W (kWh/kg)	5045	675	5250	2100
Current density $i=40$ A/m ² , temperature $T=40C^\circ$ and $[U]=25$ g/L				

Compared to stainless steel, aluminum is by far the best cathodic material tested, inducing a considerable improvement in both current efficiency and energy consumption, evidenced in a seven-fold increase in current efficiency, and a massive reduction in energy consumption (from 5045 kWh/kg to 675 kWh/kg). Contrary to what is observed for aluminium, Monel performs almost identically to stainless steel, with current efficiencies of 10.15% and 6.83% respectively and energy consumptions of 5045 kWh/kg and 5250 kWh/kg. In a similar comparison, Inconel

displays an intermediate behaviour between that observed for stainless steel and Monel, with a current efficiency of 17.07% and an energy consumption of 2010 kWh/kg.

To delve further into the behaviour observed for the data in Table 1, cathodic polarization measurements were performed. After data collection of four cathodic polarization curves, using the different electrodes, the average polarization curves obtained (Fig. 7) show that the resting potential for the cathodes considered are -0.10 V for stainless steel and Inconel, followed by Monel with -0.48 V, and aluminium showing the largest potential magnitude with -0.89 V.

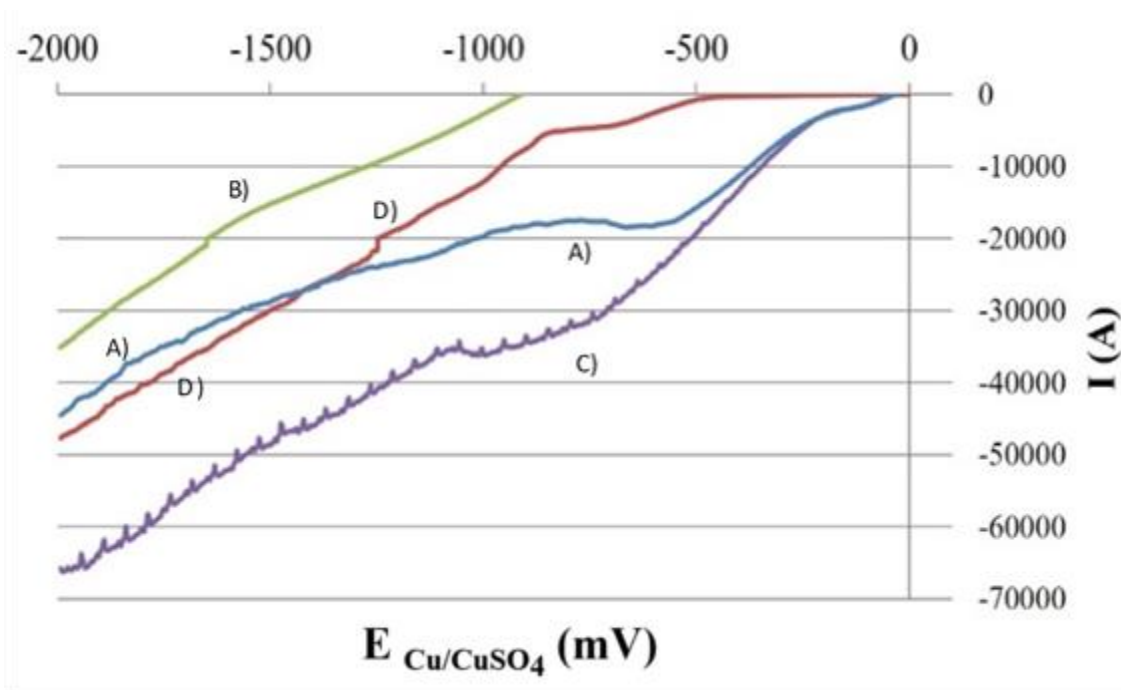


Figure 7. Cathodic polarization curve. (A) Stainless steel, (B) Aluminum, (C) Inconel, (D) Monel.

From the data shown in Fig. 7, the polarization curve of the aluminium reveals that this material has the resting potential that most closely approaches the uranium reduction potential [34], required for the studied electrodeposition process. Therefore, most of the system energy goes to the production of UF_4 , and not gaseous hydrogen. A considerable release of gaseous hydrogen is

observed when the stainless-steel cathode is used, mainly due to the H^+/H_2 reaction being catalysed by the stainless steel, inducing an increase in the acid consumption rate, devoting most of the energy consumed by the system in the hydrogen reduction reaction..

To verify that the electrodeposited material is in fact UF_4 , 2 g of the solid were sampled using X-ray mass diffraction. The diffractogram provided by the X-ray system software is shown in Figure A1 (refer to Appendix 1) with signals for the electrodeposited samples and standard UF_4 signals. The X-ray mass diffraction shows that the sample contains UF_4 and minor impurities that could not be identified to any associated by-product.

5. CONCLUSIONS

Based on the findings presented, regarding the performance of the reactive electro-electrodialysis system considered for the electrodeposition of UF_4 , the conclusions can be best summarized when the metallic cathodes considered (stainless steel and aluminum) are compared. For stainless steel, the maximum current efficiency was 10,15%, almost seven times lower than that observed when aluminum is considered (68, 29%). The performance of stainless-steel cathodes can be somewhat improved by moderately increasing the catholyte temperature (40 °C) and the uranium concentration (25 g/L). The use of aluminum cathodes involves less energy expenditure per kilogram of Uranium (675 kWh/kg U). Similarly, the release of gaseous hydrogen is significantly lower for aluminum, due to its lower exchange current density (i_0), with a magnitude of 10^{-7} A/m². On the contrary, a considerable release of gaseous hydrogen is observed when the stainless-steel cathode is used, mainly due to the H^+/H_2 reaction being catalysed by the stainless steel, inducing an increase in the acid consumption rate, devoting most of the energy consumed by the system in the hydrogen reduction reaction. Polarization cathodic curves indicate that uranium has an

estimated resting potential close to that of aluminium, which is -0.89 V. Zinc alloy cathodes (Monel and Inconel) show intermediate performance between that of stainless steel and aluminium, with Inconel being the alloy with the best relative performance.

ACKNOWLEDGEMENTS

The authors acknowledge with thanks the support given to this work by the Departamento de Materiales Nucleares of the Comisión Chilena de Energía Nuclear (CCHEN) and by the Universidad de Santiago de Chile, DICYT 021841PL and USA1899 – VRIDEI 051914 CM_PAP, Vicerrectoria de Investigación, Desarrollo e Innovación and the projects Red CYTED318RT0551 and ERAMIN 2 from ANID and European Union.

REFERENCES

- [1] E.H.P Cordfunke (1969) The chemistry of uranium. Elsevier publishing company. Netherlands
- [2] Jamie M. Purkis, Phil E. Warwick, James Graham, Shaun D. Hemming, Andrew B. Cundy (2021) Towards the Application of Electrokinetic Remediation for Nuclear Site Decommissioning, Journal of Hazardous Materials. 125274.
- [3] Esteban Duque, A., Gispert Benach, M., Hernandez Arroyo, F., Montes Ponce de Leon, M., & Rojas de Diego, J. L. (1974). F₄U production by electrolytic reduction (JEN--278). Spain.
- [4] Bonini, A., Cabrejas, J., De Lio, L., Dell'Occhio, L., Devida, C. Dupetit, G. Falcón, M. Gauna, A. Gil, D., Guzmán, G. Neuringer, P. Pascale, A. Stankevicius, A. 1998. Nuclear fuel cycle head-enriched uranium purification and conversion into metal. International Reduced Enrichment for Test Reactor Conference, Sao Paulo, Brazil.
- [5] Paulillo, A., Dodds, J., Palethorpe, S., Lettieri, P (2021) Reprocessing vs direct disposal of used nuclear fuels: The environmental impacts of future scenarios for the UK, Sust Mat Technol 28, e00278.
- [6] INTERNATIONAL ATOMIC ENERGY AGENCY (2000) Methods of Exploitation of Different Types of Uranium Deposits, IAEA-TECDOC-1174, IAEA, Vienna.
- [7] Yingcai Wang, Xue Dong, Yunhai Liu, Yuhui Liu, Xiaohong Cao, Jing Chen, Chao Xu (2020) Electrochemical and spectrochemical analysis of U(VI) reduction in nitric acid solutions, Journal of Electroanalytical Chemistry 874, 114482.
- [8] F. Valdivieso, M. Pijolat, M. Soustelle, J. Jourde. Aug-2000. Reduction of uranium oxide U₃O₈ into uranium dioxide UO₂ by ammonia. Solid State Ionics 141-142, 117-122.
- [9] Jin, W., Du, H., Zheng, S., Zhang, Y. (2016) Electrochemical processes for the environmental remediation of toxic Cr(VI): A review. Electrochimica Acta 191, 1044-1055.

- [10] Jin, W., Zhang, Y. (2020) Sustainable electrochemical extraction of metal resources from waste streams: from removal to recovery. *ACS Sustainable Chem. Eng.* 8, 4693-4707.
- [11] Mejía, R., Maturana, A., Gomez, D., Quintero, C., Arismendy, L., Cardenas, C. (2020) reuse of manganese sulfate as raw material by recovery from pesticide wastewater using nanofiltration and electro-electrodialysis: process simulation and analysis from actual data. (in press) *Water Sci. Technol.* <https://doi.org/10.2166/wst.2020.179>
- [12] Cifuentes, G. et al (2009). Copper Electrowinning Based on Reactive electro dialysis. *Journal of the Chilean Chemical Society*, Vol. 54, n° 4, 289-293.
- [13] Garrido B, Cifuentes G, Fredes P, Pino E, Calderón C and Cifuentes-Cabezas M (2021) Copper Recovery From Ammonia Solutions Through Electro-Electrodialysis (EED). *Front. Chem.* 8:622611. doi: 10.3389/fchem.2020.622611
- [14] Liu, Y., Ke, X., Zhu, H., Chen, R., Chen, X., Zheng, X., Jin, Y., Van der Bruggen, B. (2020) Treatment of raffinate generated via copper ore hydrometallurgical processing using a bipolar membrane electro dialysis system, *Chem Eng J.* 382, 122956.
- [15] Chapotot, A., Lopez, V., Lindheimer, A., Aouad, N., Gavach, C. (1995) Electro dialysis of acid solutions with metallic divalent salts: cation-exchange membranes with improved permeability to protons. *Desalination* 101, 141-153.
- [16] Jiang, C., Wang, Y., Wang, Q., Feng, H., Xu, T. (2014) Production of lithium hydroxide from lake brines through electro-electrodialysis with bipolar membranes (EEDBM). *Ind. Eng. Chem. Res.* 53, 6103-6112.
- [17] Miao, Z., Pei, F., Liu, Z., Zhang, Z., Yu, R., Liu, R. (2016) Preparation of highly purity Tetrabutyl Ammonium Hydroxide using a novel method of Electro-Electrodialysis: The study on mass transfer process and influencing factors. *J Membr Sci* 567, 281-289. <https://doi.org/10.1016/j.memsci.2018.09.045>
- [18] Pisarska, B., Jaroszek, H., Mikołajczak, W., Nowak, M., Cichy, B., Stopa, H., Markowicz, P. (2017) Application of electro-electrodialysis for processing of sodium sulphate waste solutions containing organic compounds: Preliminary study, *Journal of Cleaner Production* 142, 3741-3747.
- [19] Tanaka, N., Yamaki, T., Asano, M., Terai, Onuki, K. (2014). Membrane performance on electro-electrodialysis of HI-I₂-H₂O mixture for IS process. *Nuclear Engineering and Design*, 51-54. doi:101016/jnucengdes201311008.
- [20] Wei, Y., Wang, Y., Zhang, X., Xu, T. (2013) Comparative study on regenerating sodium hydroxide from the spent caustic by bipolar membrane electro dialysis (BMED) and electro-electrodialysis. *Sep. Purif. Technol.* 118, 1-5.
- [21] Wu, D., Chen, G., Hu, B., Deing, H. (2019) Feasibility and energy consumption analysis for phenol removal from salty wastewater by electro-electrodialysis. *Sep Pur Technol* 215. 44-50.
- [22] Yi, S., Lu, Y., Luo, G. (2008) Separation and concentration of lactic acid by electro-electrodialysis. *Sep Purif Technol* 60, 308-314.
- [23] Audinos, R. (1986) Improvement of metal recovery by electro dialysis. *J. Memb. Sci.* 27, 143-154.
- [24] V.Y. Labaton, K.D.B. Johnson (1959) The fluorides of uranium—III Kinetic studies of the fluorination of uranium tetrafluoride by fluorine, *Journal of Inorganic and Nuclear Chemistry* 10, 74-85.
- [25] Smirnov, A.L., Skripchenko, S.Y., Rychkov, V.N. et al. Preparation conditions effect on the properties of uranium tetrafluoride. *Theor Found Chem Eng* 48, 502–508 (2014).

- [26] Eykens, R., Pauwels, J., Van Audenhove, J.. The hydrofluorination of uranium and plutonium. *Nuclear Instruments and Methods in Physics Research Section A: Accelerators, Spectrometers, Detectors and Associated Equipment* 236, 497-499 (1985).
- [27] Orrego, P; Hernández, J., Puchi, F. Reduction kinetics of uranium trioxide to uranium dioxide using hydrogen. *Solid State Ionics* 101-103, 931-935.
- [28] Haynes W.M. (Ed.), *CRC Handbook of Chemistry and Physics* (97th edition.), CRC Press, Taylor and Francis, Boca Raton, FL, USA (2017)
- [29] Higgins, I.R., Roberts, J.T., Hancher, C.W., Marinsky, J.A. The Excer Process. Preparing Uranium Tetrafluoride by Ion Exchange and Electrolysis. *Ind. Eng. Chem.* 50, 3, 285–292 (1958).
- [30] Saitou, M., Teruya, S., Asadul Hossain M.S. Temperature dependence of deposition rate and current efficiency in platinum electrodeposition at a fixed average current density. *Open Electrochem. J.* 3 (2011) 1-5.
- [31] Owen, E., Jones J.I. The effect and temperature on the occlusion of hydrogen by palladium *Proc. Phys. Soc.*, 49 (1937), p. 587
- [32] Olexandra Marenych, Andrii Kostryzhev Strengthening mechanisms in nickel-copper alloys: a review *Metals*, 10 (10) (2020), p. 1358, 10.3390/met10101358
- [33] Ispas, A., Waibel, A., Fritz, M., Bund, A. (2020) Influence of Plating conditions on Nickel-Chromium Alloy Electrodeposition. *Meet. Abstr.* MA2020-02 1530.
- [34] Pourbaix, M. 1974. *Atlas of electrochemical equilibrium in aqueous solutions*. National association of corrosion engineers Eds. Texas, USA.

Appendix 1. Electronic supplementary Information for:

Tetra-uranium fluoride electrowinning by electro-electrodialysis cell (EED)

Gerardo Cifuentes¹, Ignacio Germain², Belén Garrido¹, Magdalena Cifuentes-Cabezas³,
Pedro Orrego², Iván Genticó¹, Eduardo Pino⁴, Cristian Calderón⁴

Item	Page
<i>Figure A1. X-ray diffractogram of the studied UF₄ samples</i>	3

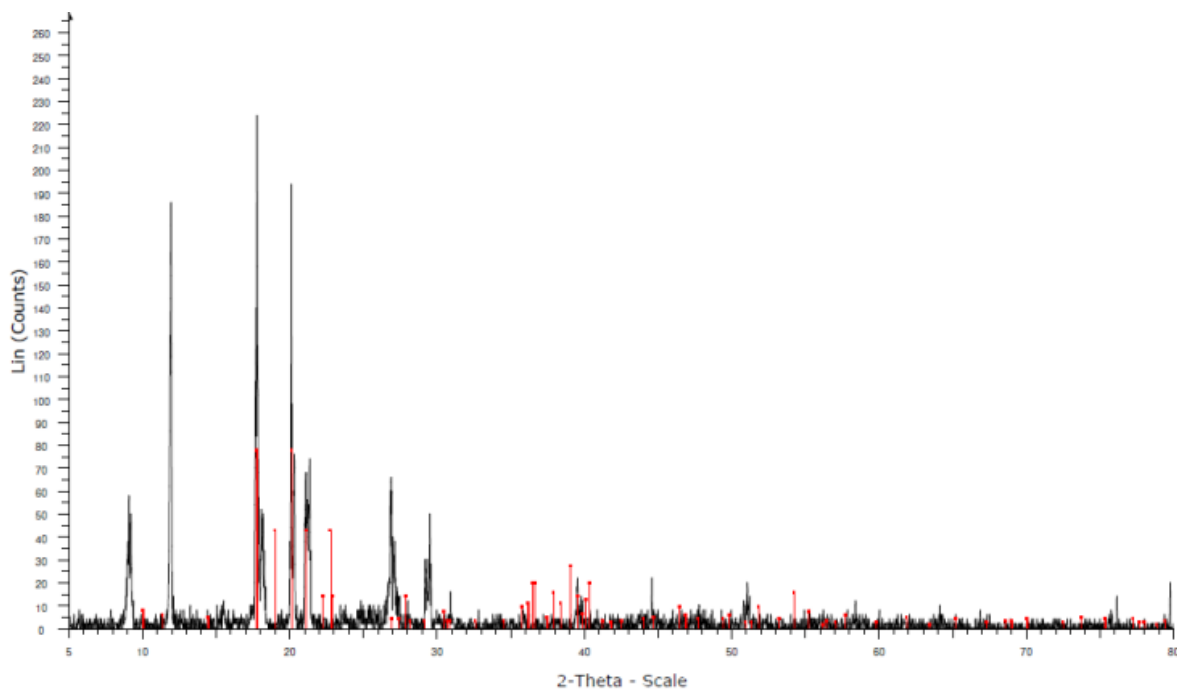


Figure A1. X-ray diffractogram of the studied UF₄ samples